

Fluid Interfaces in the 3D Ising Model as a Dilute Gas of Handles

M. Caselle¹, F. Gliozzi¹ and U. Magnea^{1,2} *

¹*Dipartimento di Fisica Teorica dell'Università di Torino
Istituto Nazionale di Fisica Nucleare, Sezione di Torino
Via P. Giuria 1, I-10125 Turin, Italy*

²*Department of Physics
State University of New York at Stony Brook
Stony Brook, New York 11794*

Abstract

We study the topology of fluid interfaces in the 3D Ising model in the rough phase. It turns out that such interfaces are accurately described as dilute gases of microscopic handles, and the stiffness of the interface increases with the genus. The number of configurations of genus g follows a Poisson-like distribution. The probability per unit area for creating a handle is well fitted in a wide range of the inverse temperature β near the roughening point by an exponentially decreasing function of β . The procedure of summing over all topologies results in an effective interface whose squared width scales logarithmically with the lattice size.

*e-mail: caselle, gliozzi, u_magnea@to.infn.it

1 Introduction

The properties of interfaces in 3D statistical systems have been a long-standing subject of research. One of the main reasons for this continuous interest probably lies in the fact that the physics of fluid interfaces can be very accurately described by field theoretic methods. Moreover, since interfaces are essentially two-dimensional objects, one is mainly interested in 2D quantum field theories (QFT), a context in which significant improvements and new understanding have been achieved during the last few years (see, for instance, ref. [1] for a comprehensive review). In particular it is by now generally accepted that the infrared (long range) properties of fluid interfaces are well described by a 2D, massless, free bosonic field theory. The bosonic field $h(x_1, x_2)$ is usually associated to the displacement of the interface from the equilibrium position as a function of the longitudinal coordinates x_1 and x_2 . This description can be obtained following a so called Solid on Solid (SOS) approximation of the interface or, equivalently, within a capillary wave approach. The crucial assumption in both these models is that the field h must be a single-valued function of the longitudinal coordinates x_1, x_2 or, in other words, that the interface must have no overhangs and no handles.

Among the various realizations of fluid interfaces, a prominent role has been played in these last years by the 3D Ising model. The reasons for this are first that the Ising model is in the same universality class as many physical systems, ranging from binary mixtures to amphiphilic membranes [2], and second, that the Ising model, due to its intrinsic simplicity, allows fast and high statistics Monte Carlo simulations, so that very precise and discriminating comparisons can be made between theoretical predictions and numerical results.

Following this line, during the last year some high precision tests of the capillary wave model and of the consequent free bosonic QFT description have been performed [3, 4]. In all the various measurements a complete agreement was found between theoretical predictions and numerical results. In particular let us mention the analysis performed by M. Hasenbusch and K. Pinn [3] of the logarithmic growth of the interface width with the longitudinal size L_s of the interface in the rough phase (see below for details and definitions). This is indeed the simplest and most stringent prediction of the free bosonic model, being immediately related to the infrared divergence of the propagator of a free bosonic field in two dimensions. Moreover it has an appealing interpretation in terms of the Mermin-Wagner-Coleman theorem, as it is the signature of the fact that a continuous symmetry (in this case the translational invariance in the transverse direction) cannot be spontaneously broken in a two dimensional quantum field theory [5].

The impressive agreement of field theoretic predictions and Monte Carlo simulations prompted us to test the above mentioned assumption of a single valued behaviour of the interface. Indeed it is rather easy to study the genus (namely the number of handles) of the interface in the Ising model. This can be done by a straightforward application of the Euler relation (see below) in the body-centered cubic (BCC) lattice where the interface is exactly self-avoiding, but it is also possible in the case of the simple cubic lattice (see below, and in ref. [6]) through a suitable set of rules to separate the interfaces along the self-intersection lines. This last case is the most interesting one since most of the published numerical results were obtained on simple cubic lattices and a direct comparison is thus possible.

In ref. [6] we tested the assumption of a single-valued interface in the region near the critical point where the interface is expected to be almost delocalized. Surprisingly enough, we found that the assumption was apparently completely wrong, that the probability of finding interfaces without handles was almost zero, that near the critical temperature the mean number of handles was very high (even of the order of several hundred on some of the lattices studied), and moreover that it was almost exactly proportional to the mean area of the interface, thus suggesting the picture of an interface “dressed” by an huge number of microscopic handles.

The simplest way to reconcile this picture with the (now even more surprising) effectiveness of the free bosonic model in describing the interface, is to identify the field h not with the microscopic “bare” interface of the Ising model (where with this term we indicate the Peierls contours separating the two phases of the Ising model), but with the “dressed” interface, in which all the handles contribute to give an intrinsic, finite thickness to the interface.

In ref. [6] we explored some of the consequences of this picture, but it remained to understand whether such a dressed interface was a feature peculiar to the critical region or depended on the fact that all the temperatures we studied were of the same order as, or higher, than the percolation threshold. For this reason, in this paper we perform a systematic analysis of the genus dependence of various physical quantities *in the whole rough phase*. We will show that in the whole rough phase handles are present and that, similarly to what was observed in ref. [6], they are microscopic (see sect. 4.1 below). Besides this underlying common behaviour let us also stress some important differences between the present work and ref. [6]. A first important difference from the critical regime studied in ref. [6] is that at these lower temperatures the density of handles is much smaller. As a consequence, the properties of these handles and the way in which their presence affects the behaviour of the whole interface, is very well described within the approximation of an uncorrelated handle distribution (see sect. 4.2 below). Second, the interfaces that we study in the present work are still rather well localized, their mean transverse width is much smaller than the lattice size L_s which fixes their longitudinal size. Hence they can be essentially considered as two-dimensional objects. On the contrary in [6], due to the vicinity to the critical point, the interfaces were almost completely delocalized, they filled the whole lattice, their typical width being much larger than the lattice sizes in the longitudinal directions. As such they could not be considered at all as two-dimensional objects. This is precisely indicated by the L_s dependence of the mean area of the interface (see sect. 4.3 below) whose power law behaviour is almost exactly $A \sim L_s^2$ in the present case (two-dimensional surface) and was a definitely larger number ($A \sim L_s^{3.7}$) in [6].

In accordance with the above picture, we will show that agreement with the field theoretic predictions (in particular with the logarithmic law discussed above) is found only by summing over all the genera (see sect. 4.4 below). Thus the picture of an effective interface emerges, where the microscopic structure is irrelevant, and which is well described by a bosonic field theory. An important physical consequence of this analysis is that in the rough phase, but far enough from the bulk critical point so that the bulk critical length is still small, an increase of the genus of the interface corresponds to an increase of its stiffness.

Let us conclude this introduction by noticing, as a side remark, the relevance of our

results for the physics of self-avoiding surfaces; indeed the fluid interfaces [6] or, more generally, the connected boundaries of the spin clusters [7] in the Ising or percolation models are at present the only systems where surfaces of high genera can be generated and are accessible to numerical simulations. Some similarity between these systems and the behaviour of 2D quantum gravity coupled to matter with central charge $c > 1$ has been observed [8, 9].

2 Capillary wave model

The starting point of the capillary wave approach is the assumption that the long-wavelength, transverse fluctuations of the interface (i.e., the capillary waves), are described by an effective Hamiltonian proportional to the change they produce in the area of the interface

$$H/k_B T = \int_0^{L_s} dx_1 \int_0^{L_s} dx_2 \sigma(\theta) \left[\sqrt{1 + \left(\frac{\partial h}{\partial x_1}\right)^2 + \left(\frac{\partial h}{\partial x_2}\right)^2} - 1 \right] , \quad (1)$$

where the field $h(x_1, x_2)$ describes the displacement of the interface from the equilibrium position as a function of the longitudinal coordinates x_1 and x_2 , L_s is the size of the lattice in the longitudinal direction, $\sigma(\theta)$ is the (reduced) interface tension and k_B is the Boltzmann constant. We have explicitly taken into account the dependence of σ on the angle $\theta(x_1, x_2)$ which the interface forms with the crystallographic plane. More precisely, θ is defined in terms of the field h as¹:

$$\theta = \arctan \left(\frac{d h}{d x} \right) \quad (2)$$

The θ dependence becomes irrelevant near the critical point, where the bulk correlation length is large and rotational invariance is restored, but it turns out to be rather important in the remaining part of the rough phase, where it survives in the thermodynamic limit. The important parameter in this phase is the *stiffness* k defined as:

$$k = \sigma(0) + \frac{d^2 \sigma}{d \theta^2} \Big|_{\theta=0} . \quad (3)$$

In the limit $\beta \rightarrow \beta_c$ the θ dependence is negligible and $k \rightarrow \sigma(0)$.

The interface free-energy increment due to interface fluctuations is then given by

$$F_{cw} = -k_B T \log \text{tr} e^{-H/k_B T} , \quad (4)$$

The Hamiltonian of eq. (1) is too difficult to be handled exactly. However, a crucial observation is that this theory can be expanded in the adimensional parameter $(kL_s^2)^{-1}$ and the leading order term is, as anticipated, the Gaussian model. Then we replace eq. (1) with the $kL_s^2 \rightarrow \infty$ limit $H \rightarrow H_G$:

¹In principle one would expect two different angles θ_1 and θ_2 for the two directions x_1, x_2 , but here and in the following we assume a complete symmetry between the two longitudinal directions. This is justified since the two directions are equivalent on the $L_s^2 \times L_t$ lattice we use.

$$H_G/k_B T = \frac{k}{2} \int_0^{L_s} dx_1 \int_0^{L_s} dx_2 \left[\left(\frac{\partial h}{\partial x_1} \right)^2 + \left(\frac{\partial h}{\partial x_2} \right)^2 \right] . \quad (5)$$

One of the most interesting predictions of the Gaussian model concerns the average surface width W , defined by

$$W^2 = \frac{1}{2L_s^4} \int_0^{L_s} d^2x \int_0^{L_s} d^2x' \langle (h(x_1, x_2) - h(x'_1, x'_2))^2 \rangle . \quad (6)$$

As is well known, in the gaussian limit the square of the interfacial width grows logarithmically as

$$W^2 = \frac{\beta_{eff}}{2\pi} \log(L_s) + C_0 \quad (7)$$

where C_0 is a constant and the "effective temperature" β_{eff} coincides in this limit with the inverse of the stiffness:

$$k = \frac{1}{\beta_{eff}} . \quad (8)$$

According to the widely accepted conjecture that the interface models near the roughening transition belong to the universality class of Kosterlitz and Thouless, it is expected that at the roughening point $\beta_{eff} = \frac{2}{\pi}$.

3 The simulation

We studied the 3D Ising model defined by the partition function

$$Z = \sum_{s_i = \pm 1} e^{-\beta H} \quad (9)$$

with the standard Hamiltonian, with nearest neighbour interaction only,

$$H = - \sum_{\langle i, j \rangle} s_i s_j , \quad (10)$$

using a cluster algorithm. We chose a simple cubic geometry whose drawback is that it does not allow a simple evaluation of the genus of the interface, but which has the important advantage that several properties of the model are known with very high precision. In particular the Ising model is known to have a second order bulk phase transition at $\beta_c = 0.221652(3)$ and a roughening transition at $\beta_r = 0.4074(3)$ [10, 3].

The simulations were performed on a $L_s^2 \times L_t$ lattice, with L_s (L_t) the lattice spacing in the longitudinal (transverse) direction. We chose periodic boundary conditions in the longitudinal directions and *antiperiodic* in the transverse direction. This forces the formation of an odd number of interfaces in this direction (actually, in almost all our configurations only one interface was present). We fixed $L_t = 32$, which in the range of β that we studied is always much larger than the mean interface width W . We did two different sets of measurements. First we systematically studied the formation of interfaces in the rough phase, choosing a rather small value of the longitudinal lattice spacing: $L_s = 14$, but keeping high statistics (20,000 measurements for each value of β)

and a very fine resolution in β . In particular, in order to better describe the region near the critical point, we chose a finer resolution close to β_c . A simple way of doing this is to choose a constant resolution $\Delta\beta_{dual} = 0.01$ in the dual coupling constant β_{dual} , defined by

$$\beta_{dual} = -\frac{1}{2} \log \tanh \beta \quad . \quad (11)$$

We studied the range $0.34 \leq \beta_{dual} \leq 0.70$ which corresponds to $0.5582 \geq \beta \geq 0.2518$. The precise correspondence between β and β_{dual} , for all the simulations we did, can be found in Table II.

Second, we selected two values of β , for which the interface was studied for varying lattice sizes L_s in the longitudinal direction. They are listed in Table I, together with the values of β_{eff} (which we shall discuss in the next section) obtained by interpolating the data reported in Table XII of ref. [3].

| β | L_s | β_{eff} |
|---------|---|---------------|
| 0.3536 | <u>14</u> , <u>16</u> , <u>18</u> , <u>20</u> , <u>22</u> , <u>24</u> , <u>48</u> | 1.45 |
| 0.3175 | <u>14</u> , 16, 18, <u>20</u> , 22, <u>24</u> , <u>32</u> , 38, <u>48</u> | 2.26 |

Table I. *Set of longitudinal lattice sizes L_s for which interfaces were studied. In the first column the corresponding values of β appears, and in the last column, the corresponding values of β_{eff} (see text) obtained in [3] are presented. For the underlined lattice sizes also the interfacial width was measured.*

In each configuration we first isolated the interface. This can be easily done by reconstructing all the spin clusters of the configuration, keeping the largest one and flipping the others. By a repeated application of this algorithm we finally eliminated all the bubbles in the configuration and obtained two pure phases, separated by one interface. We shall call the resulting configuration a “cleaned” one. Then in this cleaned configuration we measured the area A , the genus g and the width W of the interface. Let us briefly describe how these observables were measured.

Area

The area is the simplest observable to measure. Its value is given by the number of frustrated links of the cleaned configuration.

Genus

If the interface were a self-avoiding surface (and this is the case, for instance, on the BCC lattice) its genus g would be simply given by the Euler relation²:

$$F - E + V = 2 - 2g \equiv \chi(S) \quad (12)$$

where F is the number of faces (hence frustrated links in the dual framework), E the number of edges, V the number of vertices, and $\chi(S)$ the Euler characteristic

² Notice that, due to the periodic boundary conditions in the longitudinal directions, the interfaces cannot have the topology of a sphere. The simplest possible interface has the topology of a torus. This means that $g \geq 1$ and that $\chi(S)$ cannot be positive.

of the interface S . On the simple cubic lattice that we are studying this is not the case, and in general the interface has many self-intersections. We have shown in [6] how to deal with this problem and in particular we gave a local, consistent, prescription for reconstructing from the self-intersecting interface an equivalent self-avoiding surface. The term “equivalent” means that it has the same area and width. This equivalence can be stated in a rigorous, geometrical way in the framework of the Dhen lemma, which states that for any given self-intersecting surface S_1 with a self-avoiding boundary and for any real, positive ϵ , there exist infinitely many self-avoiding surfaces S_n whose distance from S_1 in the space of parameters is smaller than ϵ . Let us stress that our procedure is not unique and that in general a self-intersecting surface can be mapped into different equivalent self-avoiding surfaces, with the same area and width, but with different genus. Indeed our procedure turns out to give a consistent recipe for cutting the surface along the self-intersection lines and separating the resulting parts. These self-intersection lines are of two types: those that divide the surface in two disconnected pieces (and these can be eliminated without ambiguities), and those that do not. It can be shown that the latter give rise to a variation of the genus Δg which can take the values $\Delta g = -1, 0, 1$. This is not strange since the self-intersection lines can be thought of as separating degenerate handles from the surface. Depending on how one “cuts open” this self-intersection line to create a self-avoiding surface, these degenerate handles may either become real handles, or they may be “reabsorbed”, thus creating a “pocket” on the surface. These two possible resulting surfaces are characterized by different genus. Our reconstruction algorithm chooses between the two according to the sign of the local magnetization (for details see ref. [6]). Once a procedure for determining the genus is established one can count the number of configurations of given genus $N(g)$ in the sample. This observable will play a major role in the following analysis.

Width

The definition of the interfacial width is not unique. In order to make the comparison of results easy, we have chosen the same definition as the authors of ref. [3]. Let us define the mean magnetization in each slice in the t direction of the lattice:

$$M(t) = \frac{1}{L_s^2} \sum_{x,y=1}^{L_s} s(x, y, t) \quad (13)$$

Let us then introduce an auxiliary coordinate z for the t direction, that assumes half integer values and labels the positions between adjacent lattice layers perpendicular to the transverse direction. Let us choose the origin $z = 0$ to be in the middle of the lattice, namely between the slices located at $t = L_t/2$ and $t = L_t/2 + 1$. This means that in terms of z the above described slices of the lattice are labelled by $z = -\frac{L_t+1}{2}, -\frac{L_t-1}{2} \dots -\frac{1}{2}, \frac{1}{2} \dots \frac{L_t-1}{2}$. Let us then, following the procedure described in [3], shift the interface to the $z = 0$ position, keeping track of the antiperiodic boundary conditions. The above shift is not necessary, but reduces the spread in the measured values of the interface thickness, thereby diminishing

the noise. We can define a normalized magnetization gradient as:

$$\rho(z) = \frac{M(z + 1/2) - M(z - 1/2)}{M(-L_t/2) - M(L_t/2)} \quad (14)$$

In terms of this gradient the square of the interfacial width can be written as

$$W^2 = \left\langle \sum_z \rho(z) z^2 - \left(\sum_z \rho(z) z \right)^2 \right\rangle, \quad (15)$$

where the normalization has been chosen such that W^2 matches with the microscopic definition (7).

All the quoted errors were obtained with a standard jack-knife procedure.

4 Results

4.1 β dependence of mean area and genus

In Figs. 1 and 2 we report our results on the β dependence, at fixed value of L_s , of the genus profile and mean area of the interfaces. As expected, for large values of β (hence small temperatures) the interface is strongly constrained to the immediate neighbourhood of the crystallographic plane; the genus is always one (recall the periodic boundary conditions in the longitudinal directions), and the mean area is almost exactly that ($L_s^2 = 196$) of the crystallographic plane. As β decreases the probability of formation of handles on the interfaces in the sample increases and correspondingly also the mean area of the interface. This indicates that the fluctuations of the interface are getting larger and larger. There are some interesting properties of the interface which can be observed by studying these results:

- a] The genus of the interface is *not* an order parameter of the roughening transition. Also for $\beta > \beta_r$ we find interfaces with genus greater than 1 and their number grows as L_s increases.
- b] For any given value of β we see that the mean area of the interface increases as the genus increases. Looking at Fig. 3 one can see that the mean area differences between surfaces of genus g and $g + 1$: $\Delta A \equiv A(g + 1) - A(g)$ are essentially constant as a function of g , and grow slowly with β . This suggests to use these differences as an indicator of the mean size of a typical handle, which turns out to range from $\Delta A \sim 15 - 20$ near the roughening point, to $\Delta A \sim 25 - 30$ in the region around $\beta = 0.26$. Hence the typical handle is microscopic with respect to the size of the interface. Moreover, the fact that ΔA is almost independent of g suggests that the various microscopic handles can be considered as independent and non-interacting. Thus adding a new handle, simply amounts to adding the same number ΔA of plaquettes to the surface. While the mean size of the handles increases as β decreases, the ratio $\Delta A/A$ remains almost constant in the whole rough region $\beta < \beta_r$ (see Fig. 4), thus indicating that the increase of ΔA is simply related to the overall increase of the mean area: the handles are getting “rough” just like the whole interface.

4.2 Genus distribution function

The above results suggest that, if p is the probability of having one handle, then $p^n/n!$ is the probability of having n handles, and that this probability p should be proportional to the area A of the surface. This leads us to conjecture the following ‘‘Poisson-like’’ distribution for the number of configurations of given genus $N(g)$ in the sample :

$$N(g) = C \frac{(\mu(\beta)A(g))^{g-1}}{(g-1)!} \quad (16)$$

where C is a normalization constant which does not depend on the genus g , $\mu(\beta)$ is the probability per plaquette of having a handle and, as mentioned above, due to the periodic boundary conditions the number of microscopic handles is $n = g - 1$.

In the limit $\Delta A \rightarrow 0$, in which A does not depend on g eq. (16) would exactly become a Poisson distribution:

$$N_P(g) = N_s \frac{\lambda^{g-1} e^{-\lambda}}{(g-1)!} \quad (17)$$

where N_s is the size of the sample, $\lambda = \mu A$ and $C = N_s \exp(-\lambda)$.

As can be seen by looking at Figs. 5 and 6 our data are in remarkable agreement with eq. (16). Moreover, in the samples corresponding to smaller β or larger L_s in which ΔA cannot be neglected, one can easily see that eq. (16) gives a much better agreement with the data than eq. (17). A crucial test of eq. (16), is to show that the parameter μ only depends on β and that the dependence on the lattice size L_s is completely taken into account by the area factor. This can be tested by looking at the data at $\beta = 0.3175$. As L_s increases from 14 to 48 the function $N(g)$ changes dramatically, but it is always well described by eq. (16) with the same value of the parameter: $\mu \sim 0.0012$, (see Fig. 6)³. The function $N(g)$ is thus completely determined by the parameter $\mu(\beta)$ whose values are listed in Table II and plotted in Fig. 7. The simplest hypothesis which can be made on the β dependence of μ is that it should be of the form: $\mu \propto \exp(-2\beta l_h)$, where $\exp(-2\beta)$ is the cost of frustrating one link (hence create a new plaquette in the surface) and we define l_h to be the mean size of a typical handle. This means that for consistency we expect $l_h \sim \Delta A$. It is rather interesting to notice that, even if this hypothesis is very crude, it describes surprisingly well the actual behaviour of μ , at least in the rough region. Indeed it can be seen by looking at Fig. 7 that there is a wide range of values of β , starting from the roughening point, up to $\beta \sim 0.28$ in which μ is well described by the law:

$$\mu(\beta) = \mu_0 e^{-2\beta l_h} \quad (18)$$

with $l_h \sim 14$ and $\mu_0 \sim 7.5$, and that, as expected, $l_h \sim \Delta A$. Moreover, as the critical point is approached and as ΔA increases, also l_h increases (see the smallest values of β in Fig. 7).

³ Due to the lack of statistics for higher genera, we do not quote errors for μ and l_h . In any case we estimate that an upper bound for such errors should be of the order of 5%.

| β_{dual} | β | $\mu \times 1000$ |
|----------------|---------|-------------------|
| 0.34 | 0.5582 | |
| 0.35 | 0.5448 | 0.0002 |
| 0.36 | 0.5318 | 0.0009 |
| 0.37 | 0.5192 | 0.0013 |
| 0.38 | 0.5071 | 0.0031 |
| 0.39 | 0.4953 | 0.0058 |
| 0.40 | 0.4839 | 0.0053 |
| 0.41 | 0.4728 | 0.0086 |
| 0.42 | 0.4620 | 0.0154 |
| 0.43 | 0.4515 | 0.021 |
| 0.44 | 0.4414 | 0.028 |
| 0.45 | 0.4315 | 0.036 |
| 0.46 | 0.4219 | 0.055 |
| 0.47 | 0.4125 | 0.079 |
| 0.48 | 0.4034 | 0.111 |

a

| β_{dual} | β | $\mu \times 1000$ |
|----------------|---------|-------------------|
| 0.49 | 0.3946 | 0.139 |
| 0.50 | 0.3860 | 0.182 |
| 0.51 | 0.3776 | 0.23 |
| 0.52 | 0.3694 | 0.29 |
| 0.53 | 0.3614 | 0.35 |
| 0.54 | 0.3536 | 0.45 |
| 0.55 | 0.3461 | 0.55 |
| 0.56 | 0.3387 | 0.67 |
| 0.57 | 0.3314 | 0.84 |
| 0.58 | 0.3244 | 1.00 |
| 0.59 | 0.3175 | 1.20 |
| 0.60 | 0.3108 | 1.42 |
| 0.61 | 0.3043 | 1.71 |
| 0.62 | 0.2979 | 2.02 |
| 0.63 | 0.2917 | 2.36 |
| 0.64 | 0.2856 | 2.8 |
| 0.65 | 0.2796 | 3.3 |
| 0.66 | 0.2738 | 3.8 |
| 0.67 | 0.2681 | 4.2 |
| 0.68 | 0.2625 | 4.6 |
| 0.69 | 0.2571 | 5.1 |
| 0.70 | 0.2518 | 6.0 |

b

Table II (a-b). *The probability per plaquette of creating a handle below (Tab. II a) and*

above (Tab. IIb) the roughening temperature. In the first column the values of β_{dual} appear, in the second the corresponding values of β . In the last column the values of $(\mu \times 1000)$ are reported.

Let us conclude this section by noticing that distributions of the type of eq. (16) were already proposed both in [6] and in [7]. More precisely, the following generalization of eq. (16) was proposed:

$$N(g, A) = C_g A^{b(g-1)} e^{-\mu A} \quad (19)$$

which reduces to a Poisson distribution if $b = 1$ and $C_g \propto 1/(g-1)!$. Both in [6] and in [7] (but for different reasons), values of b different from 1 were found. In [6] this was due to the fact that, as discussed above, the geometry of the problem was drastically different (and as a matter of fact the index b was a function of the lattice size L_s). In [7] a value $b = 1.25 \pm 0.01$ was found, which could indicate the presence of a new critical behaviour near β_c but, as discussed in [7], could also be due to lattice artifacts.

In order to test the possible existence of different kinds of critical behaviour we fitted the values of $N(g)$ extracted from the Montecarlo simulations also to eq. (19) keeping b as a free parameter. We found that, in general, in a given sample, a change in b can be reabsorbed by a suitable change in μ still giving an acceptable agreement between data and theoretical distribution (even if the choice $b = 1$ is the one that in almost all cases gives the best agreement). However, the values of μ obtained in this way strongly depend on the lattice size L_s . For instance, for $\beta = 0.3175$, if we set $b = 1.25$ the parameter μ changes from $\mu = 1.35$ to $\mu = 0.80$ going from $L_s = 14$ to $L_s = 48$, thus showing that such a choice of b seems to be inadequate.

4.3 L_s dependence of the mean area

For the two values of β and for all the lattice sizes listed in Table I, we measured the mean area $A(\beta, L_s)$ (see Table III and Fig. 8).

| L_s | $A, \beta = 0.3536$ | $A, \beta = 0.3175$ |
|-------|---------------------|---------------------|
| 14 | 411.7 (0.7) | 488.6 (0.8) |
| 16 | 538.9 (1.0) | 639.3 (0.8) |
| 18 | 683.5 (1.2) | 810.1 (0.6) |
| 20 | 844.6 (1.2) | 1000.6 (1.2) |
| 22 | 1022.3 (1.2) | 1211.2 (1.2) |
| 24 | 1216.3 (1.2) | 1443.6 (1.2) |
| 32 | | 2569.4 (3.4) |
| 38 | | 3623.8 (1.6) |
| 48 | 4879.1 (4.2) | 5784.2 (3.6) |

Table III. Mean interface area at $\beta = 0.3536$ and $\beta = 0.3175$.

We fitted these values with a simple power law:

$$A(L_s) = C (L_s)^\alpha \quad . \quad (20)$$

The results are reported in Table IV (see also Fig. 8):

| | $A, \beta = 0.3536$ | $A, \beta = 0.3175$ |
|------------|---------------------|---------------------|
| α | 2.0049 (11) | 2.0047 (7) |
| C | 2.079 (8) | 2.466 (6) |
| χ_r^2 | 0.67 | 0.62 |
| $C.L.$ | 64% | 74% |

Table IV. Results of fits according to the law eq. (20). In the third and the fourth rows the reduced χ^2 and confidence level of the fits are reported.

The value of α is a precise indication of the two-dimensional nature of the interfaces that we are studying.

4.4 L_s dependence of the mean width

For the two values of β and for the subset of underlined lattice sizes listed in Table I, we measured the width $W(\beta, g, L_s)$ at fixed genus (see Figs. 9a, 9b). The values are given in Table V. In listing our results in Table V we only kept those samples in which at least 50 interfaces were present⁴. Hence, by looking at the empty spaces of Table V, one can directly see the fact, already discussed above, that the range of the most likely genera for an interface moves upwards in g with the lattice size L_s and with temperature (cf. Fig. 1). Thus, for high temperature and/or big lattices, configurations with low genera are unlikely (in fact configurations with the lowest genera were no longer observed as we moved closer to the critical point), while for low temperature and/or small lattices, an interface with a high number of handles is unlikely.

| L_s | $g = 1$ | $g = 2$ | $g = 3$ | $g = 4$ | $all\ g$ |
|-------|----------|----------|----------|----------|----------|
| 14 | 0.69 (1) | 0.76 (1) | 0.84 (2) | | 0.71 (1) |
| 16 | 0.73 (1) | 0.79 (1) | 0.81 (2) | | 0.74 (1) |
| 18 | 0.76 (1) | 0.80 (1) | 0.84 (2) | | 0.77 (1) |
| 20 | 0.79 (1) | 0.83 (1) | 0.87 (1) | 0.91 (2) | 0.81 (1) |
| 22 | 0.82 (1) | 0.86 (1) | 0.88 (1) | 0.91 (3) | 0.84 (1) |
| 24 | 0.84 (1) | 0.86 (1) | 0.89 (1) | 0.89 (2) | 0.85 (1) |
| 48 | 0.98 (1) | 0.99 (1) | 0.99 (1) | 1.00 (1) | 1.00 (1) |

a

| L_s | $g = 1$ | $g = 2$ | $g = 3$ | $g = 4$ | $g = 5$ | $g = 6$ | $all\ g$ |
|-------|----------|----------|----------|----------|----------|----------|----------|
| 14 | 1.10 (1) | 1.18 (1) | 1.25(1) | 1.34 (2) | 1.43 (4) | | 1.15 (1) |
| 20 | 1.22 (1) | 1.26 (1) | 1.31 (2) | 1.35 (2) | 1.37 (2) | 1.45 (5) | 1.28 (1) |
| 24 | 1.28 (2) | 1.32 (2) | 1.36 (1) | 1.39 (2) | 1.41 (2) | 1.47 (3) | 1.35 (1) |
| 32 | 1.38 (2) | 1.38 (2) | 1.41 (2) | 1.43 (2) | 1.45 (2) | 1.47 (2) | 1.44 (2) |
| 48 | | | 1.52 (2) | 1.51 (2) | 1.54 (2) | 1.57 (2) | 1.59 (2) |

b

⁴This threshold is somewhat arbitrary, but we checked that exactly the same results were obtained setting it at 100 or 200.

Table V (a-b). *Interface width at $\beta = 0.3536$ (a); $\beta = 0.3175$ (b). In the first column is reported the longitudinal lattice size L_s . The following columns contain the square of the interface width W^2 at fixed genus. The last column contains the effective value of W^2 obtained by summing over all genera.*

We then fitted these values with the logarithmic law, eq. (7) discussed above. The results of these fits are given in Table VI. One can see that in general all these fits have rather good confidence levels, but the values of β_{eff} change remarkably with the genus. Only summing over all the genera one recovers the known value of β_{eff} [3] (see last column of Table I). Let us stress that the remarkable agreement of these numbers with those quoted by M. Hasenbusch and K. Pinn [3] (which were obtained through a completely independent method, namely a block spin renormalization approach) is an important cross-check of the reliability of our results. This behaviour of β_{eff} can be translated into the language of interface physics by using the relation (8). It implies that, as the genus of the interface increases, *also its stiffness increases*. It is also interesting to notice that there is a natural threshold in this trend: β_{eff} is always higher than the Kosterlitz-Thouless point $\beta_{eff} = 2/\pi \sim 0.64$. What happens is again that, as the genus increases and β_{eff} decreases, the probability of finding interfaces in thermodynamic equilibrium with the Ising Hamiltonian becomes smaller and smaller. This is shown by the absence of interfaces with genus higher than 4 and 6 respectively in Tabs. VI a and b.

| <i>Genus</i> | β_{eff} | C_0 | χ_r^2 |
|--------------|---------------|----------|------------|
| <i>all g</i> | 1.49 (6) | 0.09 (3) | 1.20 |
| 1 | 1.47 (6) | 0.09 (3) | 1.14 |
| 2 | 1.17 (6) | 0.27 (3) | 0.58 |
| 3 | 0.88 (8) | 0.44 (4) | 0.70 |
| 4 | 0.76 (12) | 0.53 (7) | 1.17 |

a

| <i>Genus</i> | β_{eff} | C_0 | χ_r^2 |
|--------------|---------------|-----------|------------|
| <i>all g</i> | 2.25 (10) | 0.21 (5) | 0.16 |
| 1 | 2.11 (15) | 0.21 (7) | 0.12 |
| 2 | 1.52 (15) | 0.54 (7) | 0.28 |
| 3 | 1.33 (10) | 0.69 (5) | 0.41 |
| 4 | 0.90 (13) | 0.94 (7) | 0.96 |
| 5 | 0.95 (17) | 0.94 (9) | 2.57 |
| 6 | 0.98 (26) | 0.95 (15) | 1.33 |

b

Table VI (a-b). β_{eff} and C_0 extracted from fits to eq. (7) at $\beta = 0.3536$ (a); $\beta = 0.3175$ (b). In the last column the reduced χ^2 of the fit is reported. In the first row the result of the fit keeping all the genera together is reported. In the following rows the results at fixed genus are reported.

5 Conclusion

We have studied the topology of the fluid interfaces of the 3D Ising model in the rough phase. We found that, as the temperature increase from the roughening point to the Curie transition, more and more microscopic handles are generated which are well described by a dilute gas approximation. In particular, the number of interface configurations as a function of the genus, $N(g)$, follows a Poisson-like distribution of the kind $N(g) = C \frac{(\mu A(g))^{g-1}}{(g-1)!}$, where the probability μ per unit area of creating a handle is only a function of the temperature, and is well fitted in a wide region near the roughening point by an exponentially decreasing function of β . The interface width W follows the logarithmic scaling law eq. (7) both separately for each genus, and if one sums over the genera to recover the *effective* interface. This allows one to define a genus-dependent quantity which behaves like the stiffness of the interface. An interesting feature of the stiffness defined in such a way is that it increases with the number of handles.

Acknowledgements We thank G. Gonnella, S. Vinti, M. Martellini, M. Spreafico and K. Yoshida for many helpful discussions. In particular one of us (M.C.) would like to thank M. Martellini and M. Spreafico for discussions on the relevance of the Dhen Lemma in this context. U.M. was supported in part by a fellowship from the Italian Ministry of Foreign Affairs. She thanks the University of Turin for hospitality during the completion of this work.

References

- [1] See for instance: Les Houches, Session XLIV (1988), “Fields, Strings and Critical Phenomena”, eds. E. Brè zin and J. Zinn-Justin; North-Holland (1989).
- [2] See for instance “Physics of Amphiphilic layers”, eds J. Meunier, D. Langevin and N. Boccara; Springer-Verlag (1987).
- [3] M. Hasenbusch and K. Pinn, *Physica A* 192 (1993) 342.
- [4] M. Caselle, F. Gliozzi and S. Vinti, *Phys. Lett.* **B302** (1993) 74.
- [5] M. Lüscher, *Nucl. Phys.* **B180**, (1981) 317.
- [6] M. Caselle, F. Gliozzi and S. Vinti, preprint DFTT 12/93 and *Nucl. Phys.* **B** (Proc. Suppl.) **34** (1994) 726.
- [7] V. Dotsenko, G. Harris, E. Marinari, E. Martinec, M. Picco and P. Windey, *Phys. Rev. Lett.* **71** (1993) 811; and preprint SU-Hep-4241-563 (hep-th/9401129).
- [8] M. Martellini, M. Spreafico and K. Yoshida, A generalized model for 2D quantum gravity and dynamics of random surfaces for $d > 1$, Univ. Milano/Roma preprint (1994).
- [9] J. Ambjørn and G. Thorleifsson, *Phys. Lett.* **B323** (1994) 7.
- [10] C.F. Baillie, R. Gupta, K.A. Hawick and G.S. Pawley, *Phys. Rev.* **B45** (1992) 10438.

Figure captions

Figure 1. Genus profile of the interfaces as a function of β (note the reversed scale). For each value of β , 20,000 interfaces were studied and their genus determined. For the highest temperatures (lowest β values) studied, interfaces with genus up to 40 were present. For legibility, only the curves for the first five genera are plotted, if the number of interfaces exceeds 100. The data were taken on a lattice $L_s^2 \times L_t = 14^2 \times 32$.

Figure 2. Mean area of the interfaces as a function of β for the first ten genera. Error bars have been drawn whenever their size exceeds the size of the symbol.

Figure 3. Mean area difference ΔA between interfaces of genus g and $g + 1$ as a function of β . ΔA is essentially independent of g , and is a slowly growing function of the temperature in the rough phase (the roughening point is at $\beta \approx 0.4074(3)$). For legibility of the graph, only scattered error bars have been drawn.

Figure 4. Normalized mean area difference between interfaces of genus g and $g + 1$ in the rough phase. Below the roughening point ($\beta \approx 0.4074$), $\Delta A/A$ is essentially constant as a function of β . Scattered error bars are shown.

Figure 5. Genus distributions of interfaces at varying values of β and fixed lattice size. The number of configurations with given genus g , $N(g)$ follows the Poisson-like law (16). The histograms represent the measured values of $N(g)$, while the squares are the values calculated using eq. (16), where the temperature-dependent parameter μ is given in Table II, and the measured areas were used.

Figure 6. Same as Fig. 5, but at the fixed inverse temperature $\beta = 0.3175$, and with varying longitudinal lattice size L_s . The parameter μ is always the same.

Figure 7. An illustration of the law (18) for $\mu(\beta)$, the probability per plaquette of having a handle. This law was based on the simplest possible assumption concerning the dependence of μ on β . The line is eq. (18) with $l_h \simeq 14$ and $\mu_0 \simeq 7.5$, and the squares are the values for $\log(\mu)$ extracted from (16) and the measured values for $N(g)$ (number of interfaces) and $A(g)$ (area of interfaces) at fixed lattice size as a function of β . Due to the lack of statistics for higher genera, we do not quote errors for μ .

Figure 8. Mean area A of interfaces as a function of lattice size L_s and inverse temperature β . On the horizontal axis we have $\log(L_s)$, and on the vertical axis $\log(A)$. The straight lines represent the power law fits (20) (see Table IV). The errors are microscopic on the scale of the figure. The measured points are for the effective interface (summed over all genera).

Figure 9a-b. Squared interface width W^2 versus $\log(L_s)$ at $\beta = 0.3536$ (a) and $\beta = 0.3175$. At $\beta = 0.3536$, statistics for the first four genera were available, and for $\beta = 0.3175$, for the first six. The measured values for the interface width (defined in (15)) are plotted, with fits according to eq. (7) corresponding to the dashed lines. The measured squared width of the effective interface, summed over all genera, is also shown together with the fit (the whole-drawn line). Here one gets a clear hint as to how the various topologies "sum up" to give an effective interface.

Fig. 1. Number of configurations with given genus

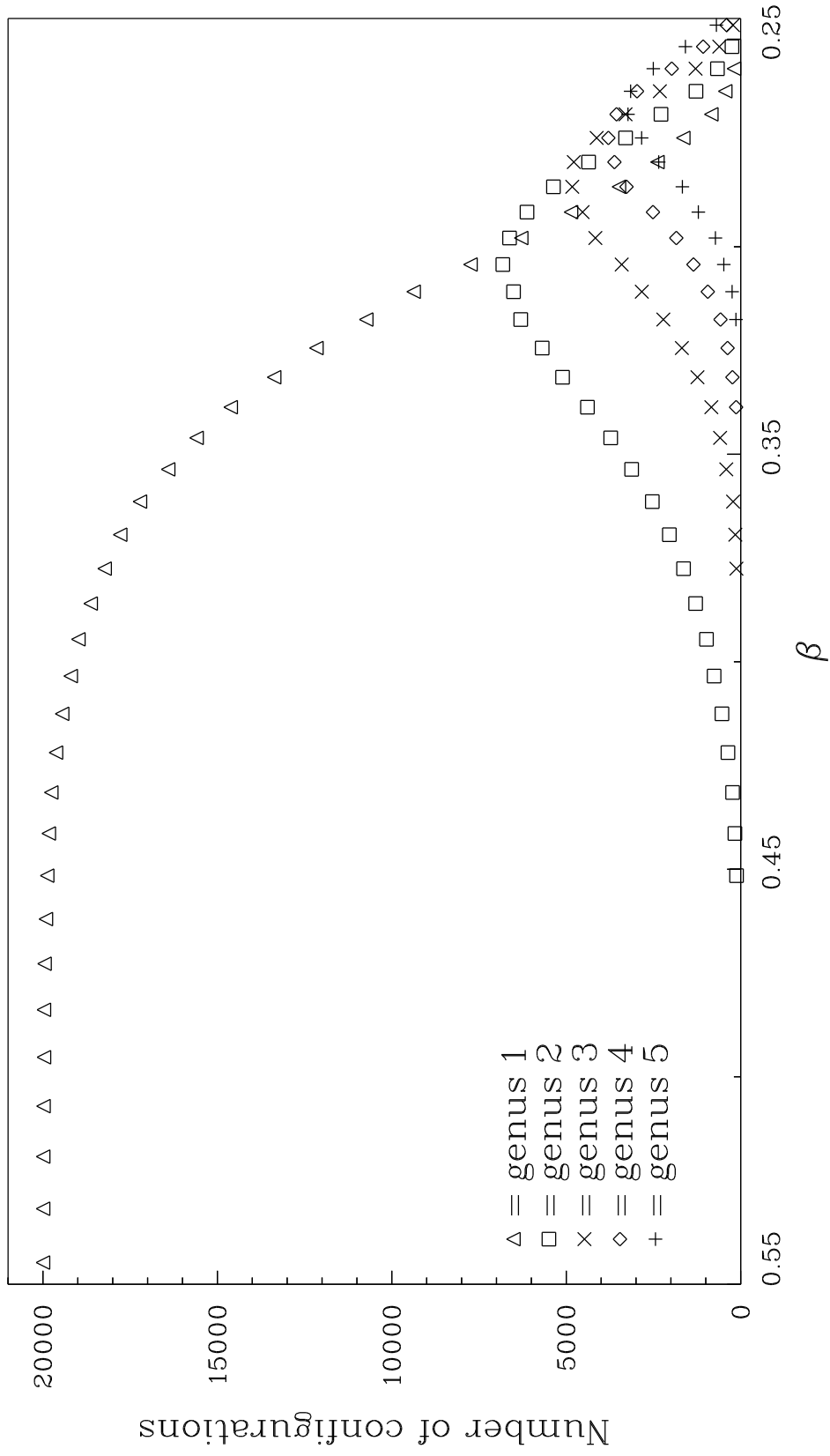


Fig. 2. Average area of interface as a function of β

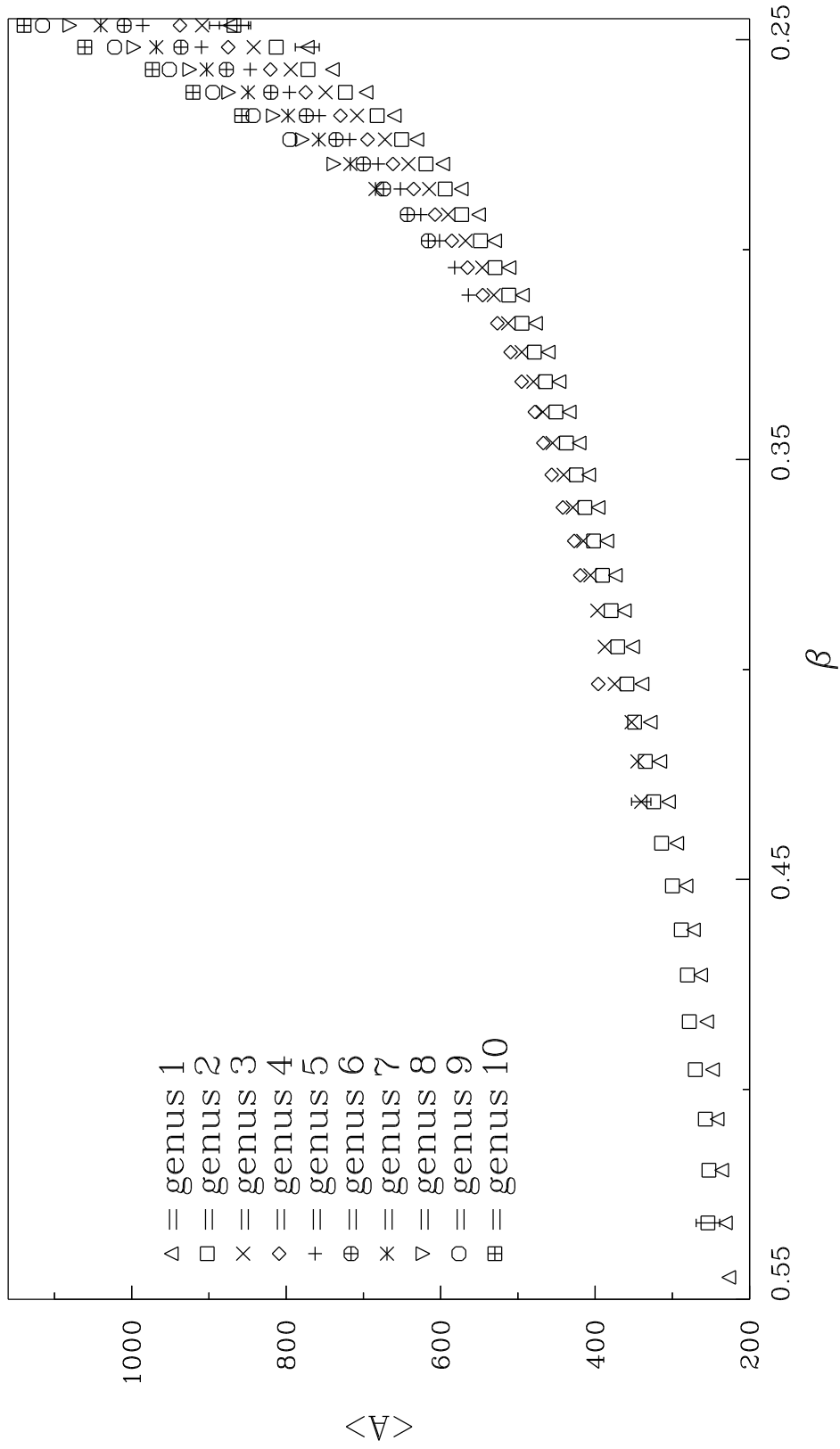


Fig. 3. Area difference as a function of β

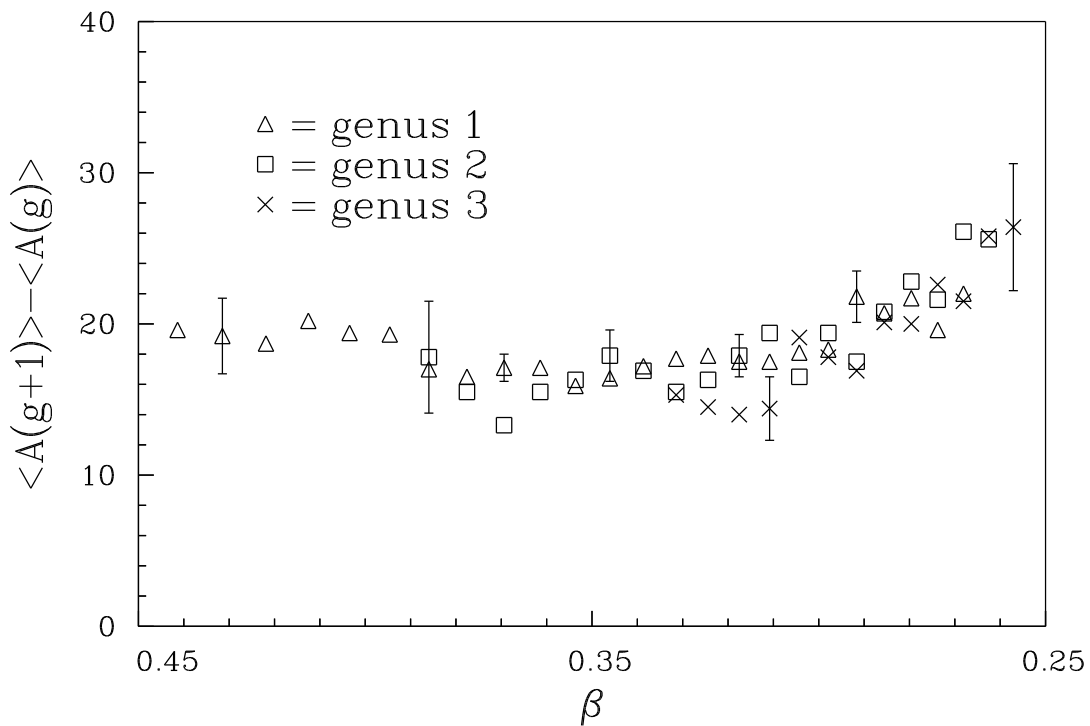


Fig. 4. Normalized area difference

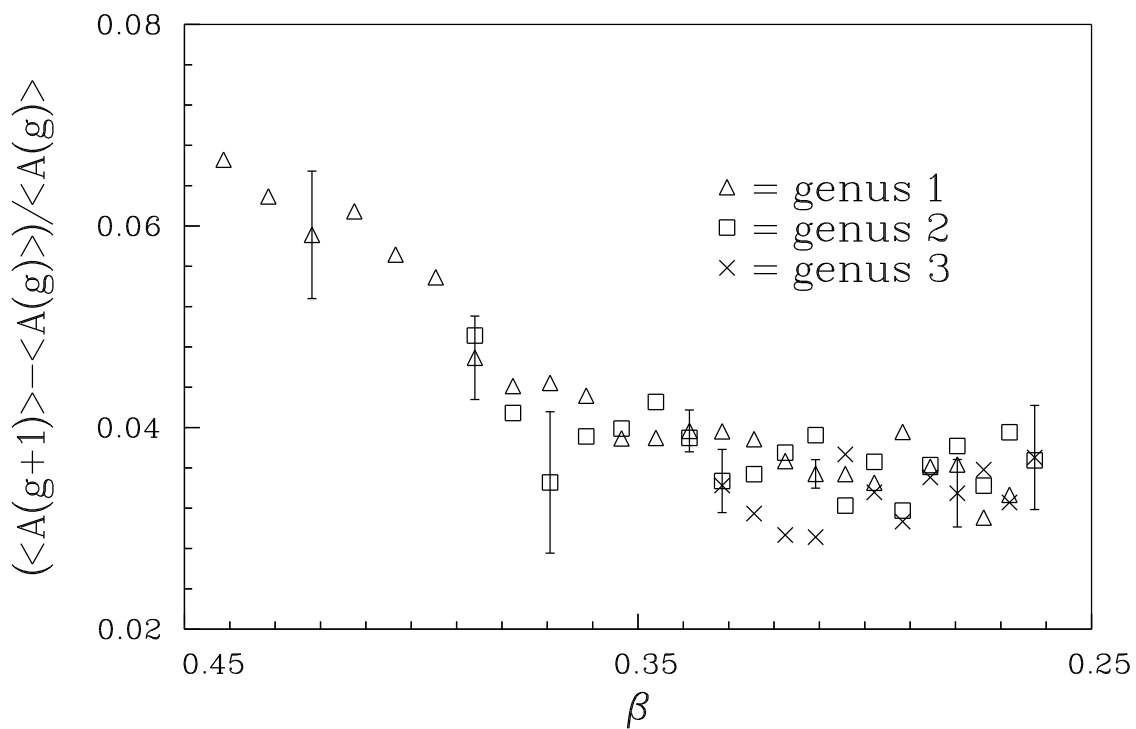


Fig. 5. Genus distributions for varying β

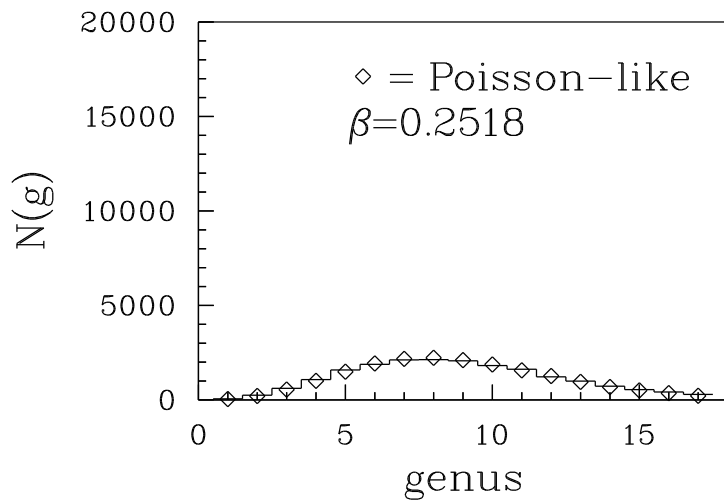
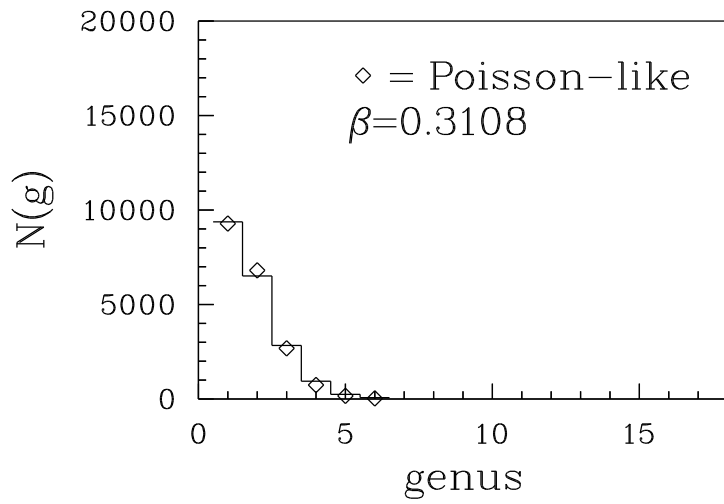
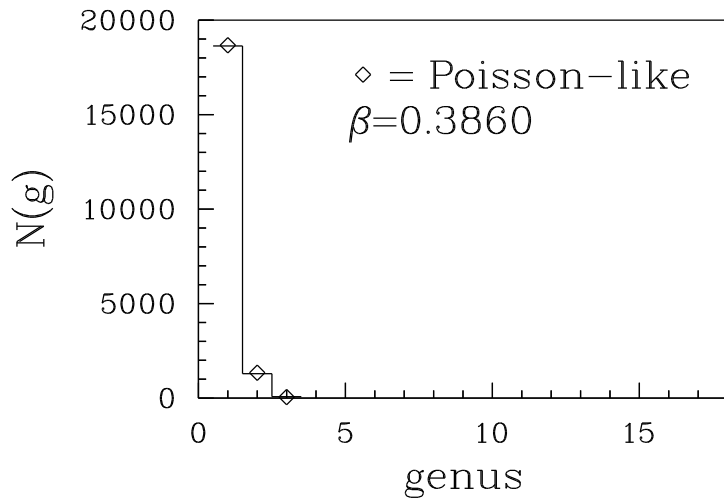


Fig. 6. Genus distributions for varying lattice size

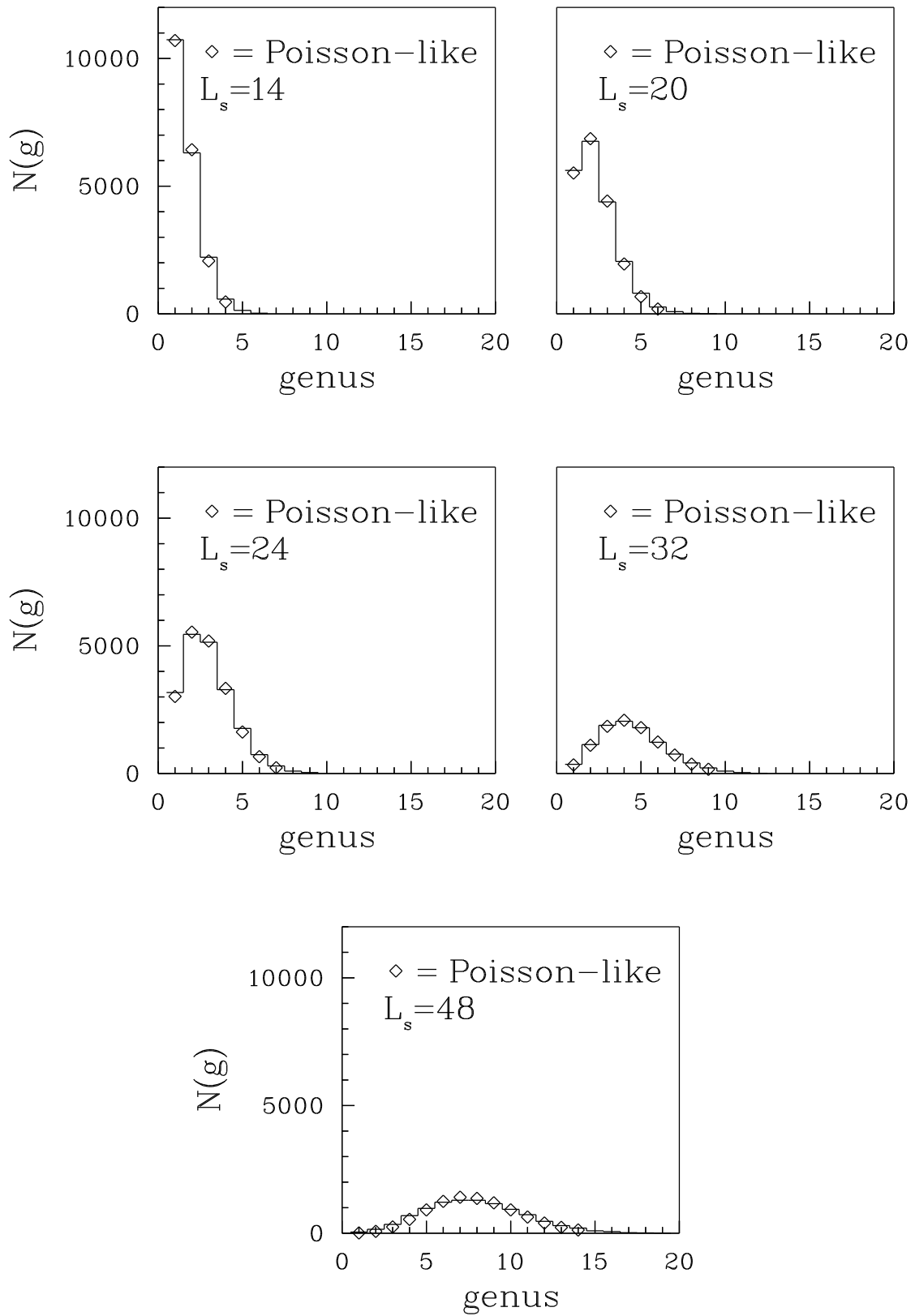


Fig. 7. Probability per plaquette of having a handle

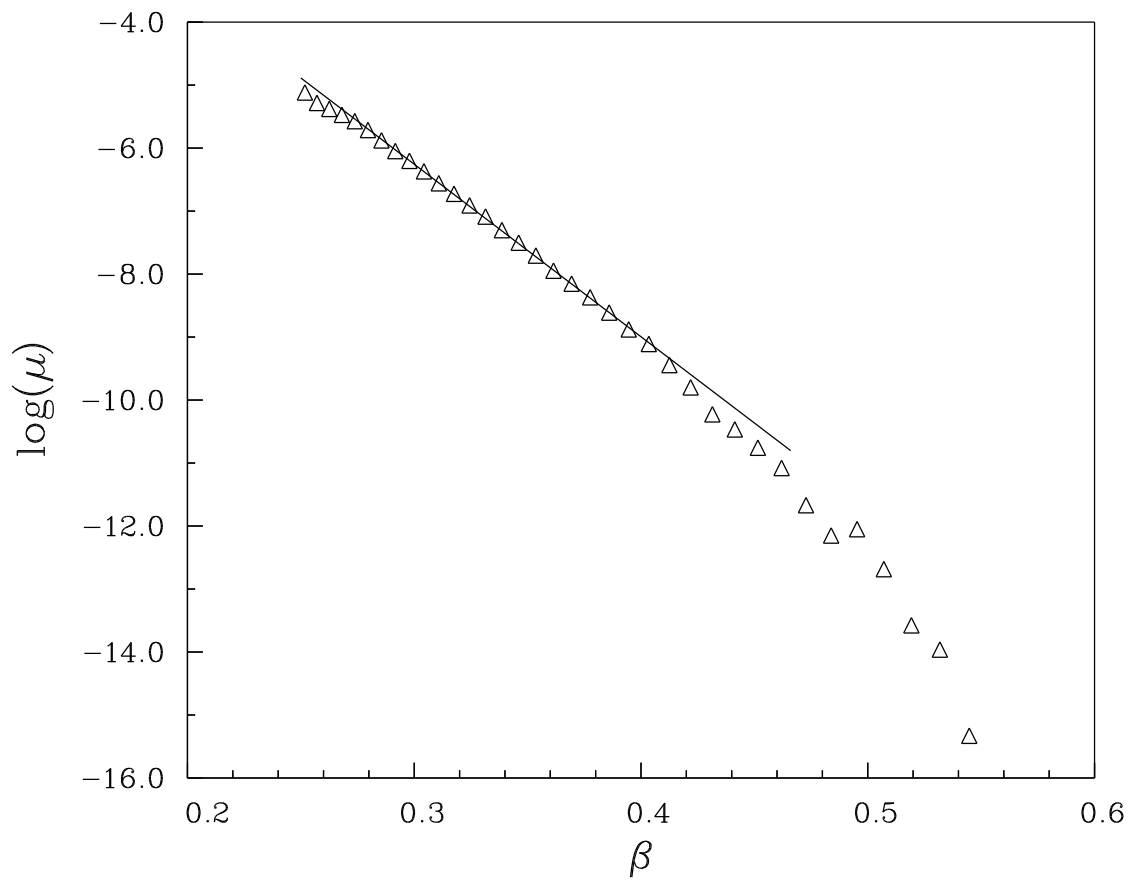


Fig. 8. Effective interfacial area

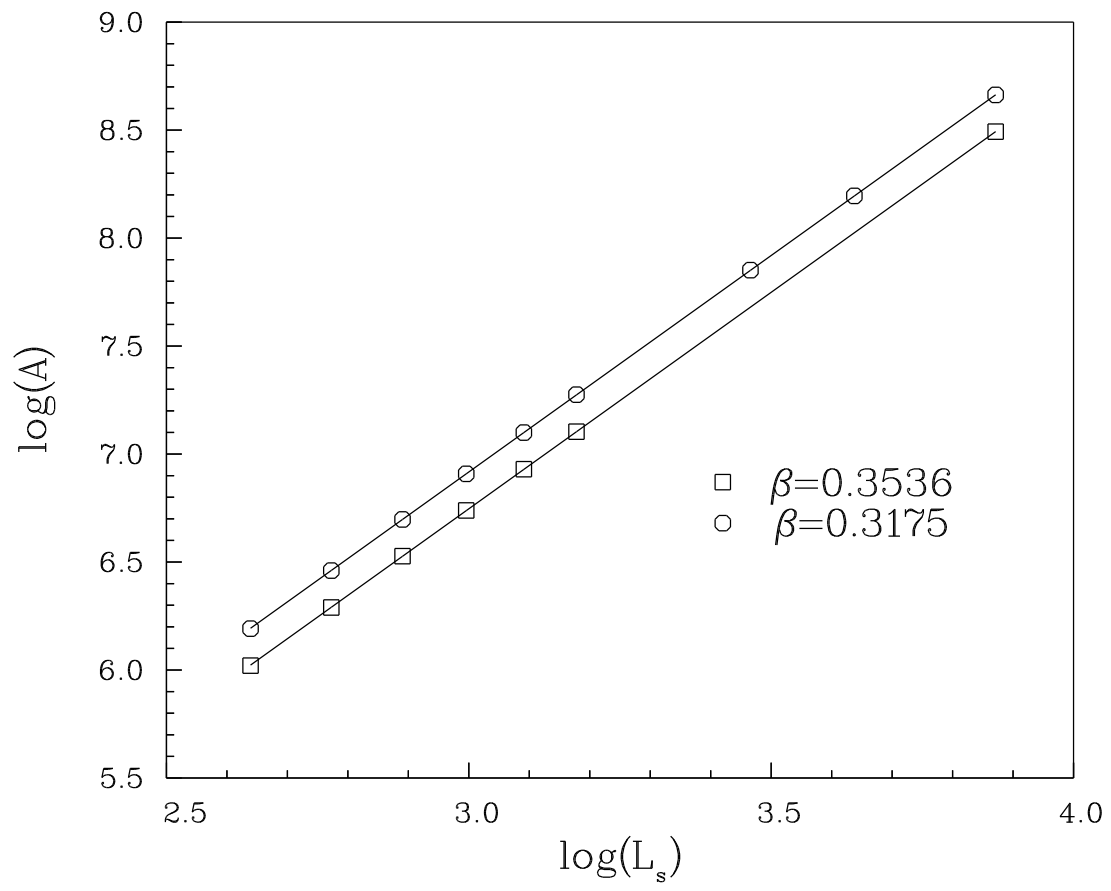


Fig. 9a–b. Interfacial width

